

Exclusive Measurements of Virtual Bremsstrahlung in Proton-Proton Scattering at 190 MeV

J. G. Messchendorp, J. C. S. Bacelar, M. J. van Goethem, M. N. Harakeh, M. Hoefman,
H. Huisman, N. Kalantar-Nayestanaki, H. Löhner, R. W. Ostendorf, S. Schadmand,*
R. Turrisi,[†] M. Volkerts, and H. W. Wilschut

Kernfysisch Versneller Instituut, Zernikelaan 25, 9747 AA Groningen, The Netherlands

R. S. Simon

Gesellschaft für Schwerionenforschung, Planckstraße 1, D-64291 Darmstadt, Germany

A. Kugler and V. Wagner

Nuclear Physics Institute, 250 86 Řež u Prahy, Czech Republic

(Received 25 September 1998)

Exclusive differential cross sections of virtual bremsstrahlung in proton-proton scattering below the pion-production threshold have been measured for the first time. The total cross section integrated over photon invariant masses of 15 to 80 MeV/ c^2 and integrated over the acceptance of the detector is $3.2 \pm 0.1 \pm 0.5$ pb. The data are compared to a low-energy calculation and a fully relativistic microscopic model, which predict a virtual bremsstrahlung cross section of 3.4 and 5.9 pb, respectively. Over the entire experimentally covered phase space, the low-energy calculation gives a better description of the data than the microscopic model. [S0031-9007(99)08793-1]

PACS numbers: 13.75.Cs, 25.10.+s, 25.20.Lj

The study of real-photon bremsstrahlung emission during proton-proton collisions below pion-production threshold has recently received a large boost. High-quality, intense, polarized-proton beams together with high-precision detection equipment have provided accurate exclusive cross sections and polarization measurements [1,2]. With the presently achieved accuracies, one is sensitive to details of the nucleon-nucleon interaction. State-of-the-art calculations [3–6] are now relativistic, showing the sensitivity to negative-energy states, and include non-nucleonic degrees of freedom such as the virtual excitation of the Δ and meson-exchange currents.

The emission of virtual bremsstrahlung ($p + p \rightarrow p + p + \gamma^* \rightarrow p + p + e^+ + e^-$), on the other hand, has up to now not been investigated. The difficulty in the experimental study of this process arises from the fact that the cross section is lower by approximately a factor of $\alpha = 1/137$, the fine-structure constant, than the already small cross section for bremsstrahlung associated with real-photon emission. The measurement of virtual photons allows the decomposition of the nucleon current into transverse and longitudinal components as well as interference terms, the so-called nucleonic response functions. Furthermore, the nucleon-nucleon- γ^* vertex is measured in the timelike region. Calculations predict a large sensitivity of the nucleonic response functions to the details of the nucleon-nucleon interaction [7].

In this paper we present the first measurements of the virtual bremsstrahlung cross section. These studies, performed at 190 MeV, obtained a total of 600 background-free ppe^+e^- events. The angular distribution of virtual photons as well as the invariant-mass dependence was determined. The data are compared with predictions based

on a relativistic low-energy theorem [8,9], as well as a relativistic microscopic calculation by Martinus *et al.* [7]. Within the experimental accuracy and phase-space coverage, the data are in rather good agreement with the calculation based on the low-energy theorem, which gives a cross section integrated over the experimentally covered phase space of 3.4 pb. The microscopic model seems to overestimate the experimental cross section, with a predicted cross section for virtual bremsstrahlung of 5.9 pb.

The experiment was performed at the Kernfysisch Versneller Instituut (KVI) using a 190 MeV polarized-proton beam provided by the superconducting cyclotron AGOR. A cylindrically shaped (6 mm thick and 20 mm diameter) liquid-hydrogen target [10], with 4 μ m thin Aramid windows, was used with an average beam current of 6 nA. Under these conditions data were taken for a period of approximately 200 hours. The two protons and two leptons were measured in coincidence using the Small-Angle Large-Acceptance Detector (SALAD) and the Two-Arm Photon Spectrometer (TAPS), respectively. The experimental setup is illustrated in Fig. 1.

SALAD [2] consists of two wire chambers and 24 plastic scintillators allowing one to measure the scattering angle of the two outgoing protons in the range $6^\circ < \theta_p < 19^\circ$ with full coverage of the azimuthal angle ϕ and up to 26° for a reduced range of ϕ angles. SALAD determines the position and energy with an angular resolution of 0.5° and an energy resolution of about 5%. To reduce the trigger rate [11] of the elastic channel, 26 thin plastic scintillators were placed behind the energy scintillators and used as veto detectors. The TAPS detector [12], consisting of 384 BaF₂ crystals, has been divided up into 6 closely packed blocks, each containing 64 crystals. These

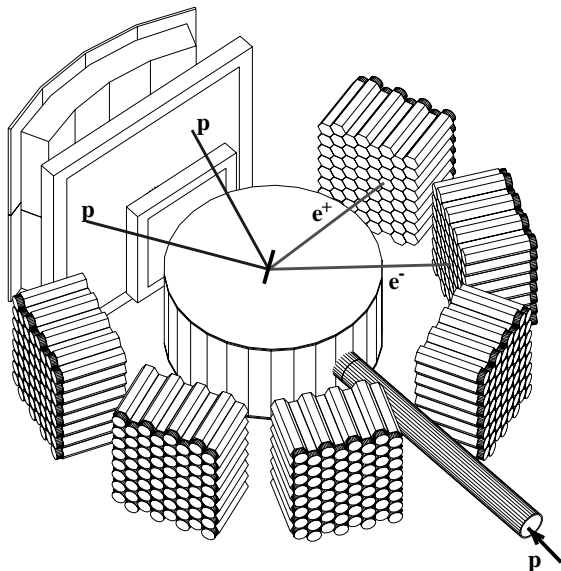


FIG. 1. Schematic view of the experimental setup consisting of SALAD (two wire-chambers and 50 plastic scintillators) and TAPS (384 hexagonal BaF_2 crystals). Not drawn are the thin plastic scintillators placed in front of each BaF_2 crystal. An example of a $pp e^+ e^-$ event originating from the liquid-hydrogen target is indicated.

blocks are placed around the target position in the median plane at polar angles of 76.5° , 116.5° , and 156.5° at a distance of 66 cm from the target, resulting in a coverage of the polar angle of the virtual photon between 60° and 180° and providing the possibility to detect photons with large invariant masses up to the kinematical limit of $93 \text{ MeV}/c^2$. Furthermore, in front of each BaF_2 crystal, a 5 mm thick plastic scintillator is mounted in order to distinguish between charged (electrons and positrons) and neutral particles (photons).

In the experiment, the positions and total energies of all four outgoing particles are measured (i.e., 12 observables). Since there are only 8 independent variables in the outgoing channel, our measurements are kinematically overdetermined. Prompt-time coincidence events with two proton candidates (two charged-particle tracks in SALAD) and two lepton candidates (two charged electromagnetic showers in TAPS) are selected. Only lepton pairs for which the showers are not overlapping (separated by at least one crystal) are considered as candidates. This condition limits the acceptance in the opening angle of the lepton pair to $\theta_{e^+e^-} > 8^\circ$. This limitation, together with the minimum energy acceptance of our lepton detectors, sets a lower limit of $15 \text{ MeV}/c^2$ in M_γ .

Therefore, we present the data for $M_\gamma \geq 15 \text{ MeV}/c^2$. In order to make use of the kinematical overdetermination, the momenta and energies of each particle are reconstructed from the measured positions of all four particles. To reduce background, for each particle the reconstructed energy and momentum are checked against the measured

values. The measured cross section is not sensitive to small variations in the applied cuts.

The experimental acceptance for determining two protons and two leptons within the coverage of the setup and within the previously mentioned conditions relative to the total production of $pp e^+ e^-$ events is 0.1%. This result has been obtained by performing Monte Carlo simulations, using the detector simulation package GEANT3 [13] and an event generator based on a low-energy calculation [8]. The detector acceptance depends weakly on the photon invariant mass for $M_\gamma \geq 15 \text{ MeV}/c^2$; however, it primarily determines the shape of the angular distribution. Efficiencies for different detector components were measured individually by several dedicated experiments [11,14]. This includes the wire-chamber efficiency (0.851 ± 0.001 per proton) [14], trigger efficiency (0.87 ± 0.01) [11], and the TAPS plastic scintillator efficiency (0.84 ± 0.05 per lepton). All these efficiencies were as well determined by samples of data acquired concurrently with the bremsstrahlung data. Background originating from the target walls was measured by emptying the target cell of liquid hydrogen. It was found to be negligible. The contamination originating from combinatorial background, where one or more of the four coincidence particles is accidental, has been estimated by studying the time correlation between the outgoing particles, and by an event-mixing analysis. A contribution of less than 2% for all invariant masses, M_γ , is found. Another source of contamination is caused by real photons, originating from either the $p + p \rightarrow p + p + \gamma$ or the $p + p \rightarrow p + p + \gamma + \gamma$ channel. These photons induce an electron-positron pair by the process of external conversion, therefore creating two charged electromagnetic showers in TAPS. The corresponding contamination has been studied with the help of Monte Carlo simulations and is found to be negligible for the data shown in this Letter. The $pp\gamma\gamma$ process has been measured for the first time in this experiment (to be published elsewhere) and has equal or even larger strength than the $pp e^+ e^-$ reaction at some specific parts of the phase space. Because of the kinematical similarity of both processes, the use of the thin plastic scintillators (for the identification of charged particles) is essential in eliminating the contribution from the $pp\gamma\gamma$ reaction.

Differential cross sections as a function of several observables have been determined. With the use of the concurrently measured elastic channel ($\pm 1\%$ uncertainty), the experimentally determined differential cross sections are given on an absolute scale with a systematical uncertainty of $\pm 15\%$. The latter error is obtained by combining the uncertainties in the efficiencies of the individual detectors, the uncertainty in the normalization to the elastic channel, and the fluctuations in the experimentally determined bremsstrahlung cross section with respect to the elastic channel ($\pm 10\%$). In Fig. 2 the differential cross section as a function of the photon invariant mass and the

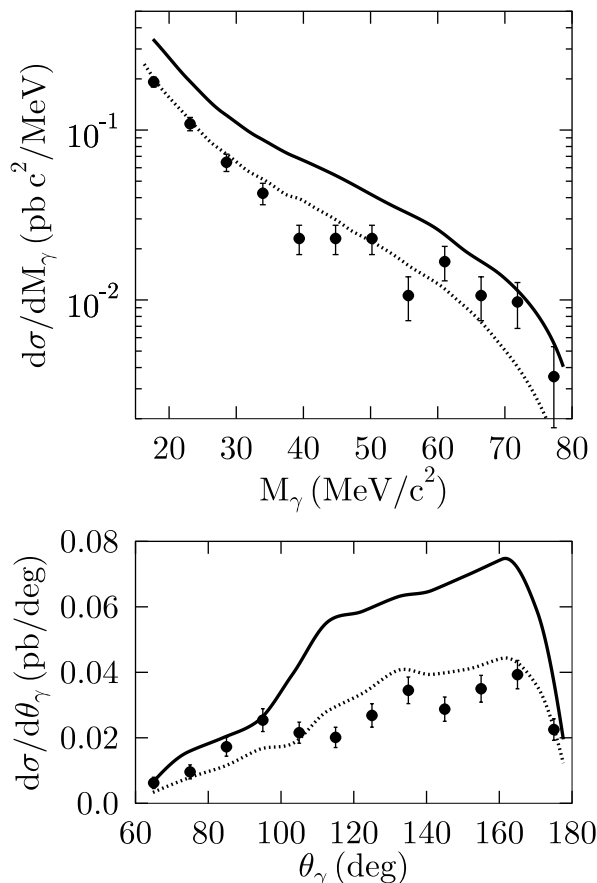


FIG. 2. Top: Differential cross section as a function of the invariant mass (M_γ) of the virtual photon integrated over the entire detector acceptance. Bottom: Virtual-photon angular distribution in the laboratory frame for invariant masses integrated from 15 to 80 MeV/c^2 . The solid lines present the results of a microscopic model and the dotted lines the results of a LET calculation. The calculations are discussed in the text. Calculations are folded with the detector acceptance.

virtual-photon angular distribution are shown. Only statistical error bars are depicted. The data are integrated over the phase space covered by the detector setup. Furthermore, the energy of the particles is restricted to $E > 5$ MeV for the leptons, $E > 20$ MeV for the protons, and $M_\gamma \geq 15$ MeV/c^2 . Under these constraints the measured cross section integrated over the covered phase space and photon invariant masses from 15 to 80 MeV/c^2 , amounts to $3.2 \pm 0.1 \pm 0.5$ pb, where the errors are statistical and systematical, respectively.

The invariant-mass distribution for two different proton-angle combinations is demonstrated in Fig. 3. In the top panel of Fig. 3, events are selected for which both proton polar angles, θ_p , are larger than 15° . The bottom panel shows the differential cross section for proton angles smaller than 15° , i.e., for large momentum transfer and consequently large photon total energy.

In both Figs. 2 and 3 the ppe^+e^- data are compared to two calculations. The first calculation, shown as the

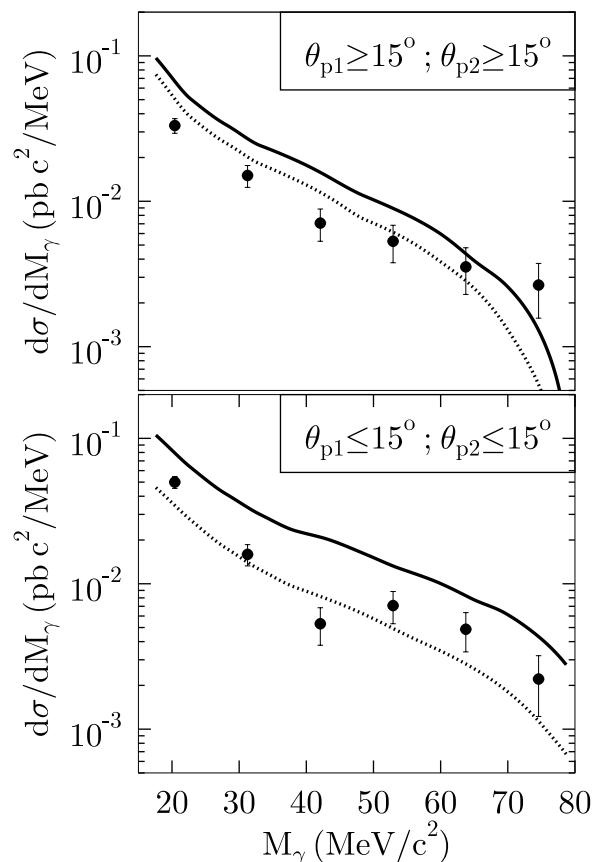


FIG. 3. Differential cross sections as a function of the invariant mass for protons with polar angle larger than 15° (top panel) and proton angles smaller than 15° (bottom panel). The solid lines present the results of a microscopic model and the dotted lines the results of a LET calculation. Calculations are folded with the detector acceptance.

solid lines, is the result of a (fully) relativistic microscopic calculation by Martinus *et al.* [7] based on the Fleischer-Tjon potential [15]. This model includes the off-shell dynamics of the intermediate protons. Furthermore, it takes explicitly into account the rescattering contributions, meson-exchange currents, and the virtual Δ -isobar.

The second calculation, shown as the dotted lines, is based on the low-energy (soft-photon) theorem (LET) derived by Korchin *et al.* [8], in analogy to the real-photon case [16]. Here, the virtual-bremsstrahlung amplitude is expressed in terms of the elastic pp process and the static properties (mass, charge, and magnetic moment) of the proton. The internal amplitude takes partially rescattering and meson-exchange currents into account and is obtained from gauge invariance. It is noted that Korchin *et al.* [8] developed on their paper two LET approaches. For simplicity we show here the one, labeled VL in [8], which clearly fits our data the best. The second approach lies approximately 20% higher.

To compare the calculations with the data, an event generator simulating both models has been employed.

Implementation is done by using a four-body decay program [17], generating ppe^+e^- events according to phase-space distribution, and by weighting each event with the square of the reaction amplitude obtained from the calculations. The detector response is simulated using the software package GEANT3 [13]. Subsequently, the simulated weighted events are analyzed with the same software constraints as applied to the experimental data. In the angular distribution shown in the bottom panel of Fig. 2, the modulations shown by the lines represent the experimental response of the six TAPS blocks.

The state-of-the-art microscopic calculation overestimates the measured differential cross sections both as a function of the invariant mass as well as the photon angle. Since the microscopic calculation explicitly accounts for relativistic effects and different sources of non-nucleonic contributions, the observed large discrepancy points to important modifications in off-shell dynamics or equivalently to important contributions from contact terms which have not been considered.

The general trend is that within the covered phase space the microscopic model predicts approximately 50% larger cross sections than the LET calculation for the complete invariant-mass and polar-angle distribution. The total integrated and accepted cross section is 5.9 and 3.4 pb for the microscopic and LET calculation, respectively. As demonstrated in Fig. 3 the difference between the two models strongly depends on the selection in the proton angle. The difference between the two calculations becomes larger for protons with polar angles smaller than 15° as shown in Fig. 3, therefore making this part of the phase space ideal for comparing data with models. It is clear that the microscopic model needs improvement. Since the discrepancy with the present data is large, the same comment is likely to be applicable as well to the real-photon bremsstrahlung observables.

In summary, the present data show for the first time that it is possible to determine virtual-bremsstrahlung cross sections in proton-proton inelastic scattering. A total cross section integrated over the accepted phase space of $3.2 \pm 0.1 \pm 0.5$ pb has been measured. In spite of the small cross section and our small overall acceptance for this reaction channel, the virtual-bremsstrahlung yields were explored in some detail. A state-of-the-art microscopic calculation seems to overestimate the experimental cross section. The calculation based on a low-energy theorem is in better agreement with the data.

The authors acknowledge the support by the TAPS collaboration in the operation of the Two-Arm Photon Spec-

trometer at KVI and thank A. Yu. Korchin, G. Martinus, R. Timmermans, and O. Scholten for providing the computer codes for the calculations and for useful discussions. The work provided by the cyclotron and polarized-ion source group in delivering a high-quality beam was essential for the success of the experiment. This work was supported in part by the "Stichting voor Fundamenteel Onderzoek der Materie" (FOM) with financial support from the "Nederlandse Organisatie voor Wetenschappelijk Onderzoek" (NWO), by the "Granting Agency of the Czech Republic," by GSI, the German BMBF, and by the European Union HCM network under Contract No. HRXCT94066.

*Present address: Physikalisches Institut, Heinrich-Buff-Ring 16, D-35392 Gießen, Germany.

†Present address: Dipartimento di Fisica dell'Università Corso Italia, 57 95129 Catania, Italy.

- [1] K. Michaelian *et al.*, Phys. Rev. D **41**, 2689 (1990).
- [2] N. Kalantar-Nayestanaki, Nucl. Phys. A **631**, 242c (1998).
- [3] F. de Jong and K. Nakayama, Phys. Lett. B **385**, 33 (1996).
- [4] J. A. Eden and M. F. Gari, Phys. Lett. B **347**, 187 (1995); Phys. Rev. C **53**, 1102 (1996).
- [5] G. H. Martinus, O. Scholten, and J. A. Tjon, Phys. Rev. C **56**, 2945 (1997).
- [6] G. H. Martinus, O. Scholten, and J. A. Tjon, Phys. Lett. B **402**, 7 (1997).
- [7] G. H. Martinus, Ph.D. thesis, University of Groningen, 1998; G. H. Martinus *et al.*, Few-Body Syst. (to be published).
- [8] A. Yu. Korchin and O. Scholten, Nucl. Phys. A **581**, 493 (1995).
- [9] A. Yu. Korchin, O. Scholten, and D. Van Neck, Nucl. Phys. A **602**, 423 (1996).
- [10] N. Kalantar-Nayestanaki *et al.*, Nucl. Instrum. Methods Phys. Res., Sect. A **417**, 215 (1998).
- [11] S. Schadmand *et al.*, Nucl. Instrum. Methods Phys. Res., Sect. A **423**, 174 (1999).
- [12] A. R. Gabler *et al.*, Nucl. Instrum. Methods Phys. Res., Sect. A **346**, 168 (1994).
- [13] R. Brun, F. Bruyant, A. C. McPherson, and P. Zancarini, GEANT3 Users Guide, Data Handling Division DD/EE/84-1, CERN, 1986.
- [14] M. Volkerts *et al.* (to be published).
- [15] J. Fleischer and J. A. Tjon, Nucl. Phys. B **84**, 375 (1975); Phys. Rev. D **21**, 87 (1980).
- [16] F. E. Low, Phys. Rev. **110**, 974 (1958).
- [17] F. James, CERN Report No. 68-15 (1968).